

Jets in heavy ion collisions with ATLAS

Martin Spousta (for the ATLAS Collaboration)¹

Columbia University in the city of New York, Charles University in Prague

Abstract

The energy loss of high- p_T partons provides insight into the transport properties of the medium created in relativistic heavy ion collisions. Evidence for this energy loss was first experimentally established through observation of high- p_T hadron suppression at RHIC. More recently, measurements of fully reconstructed jets have been performed at the LHC. In this summary the latest experimental results from the ATLAS collaboration on jet suppression are presented. In particular the jet suppression in inclusive jet yields, path length dependence of the jet suppression, photon-jet and Z^0 -jet correlations, heavy flavor suppression, and jet fragmentation are discussed. These results establish qualitative features of the jet quenching mechanism as experimental fact and provide constraints on models of jet energy loss.

1. Introduction

Collisions of lead ions at Large Hadron Collider (LHC) are expected to create a strongly interacting matter in which quarks and gluons are locally deconfined. Jets produced in hard scattering are expected to be modified due to the energy loss of outgoing parton traversing the hot QCD medium. This effect is commonly referred to as a jet quenching. Jets therefore represent an important tool for studying both the properties of the deconfined matter and the parton energy loss [1]. In this paper we will provide a status report on jet measurements performed using the 2010 and 2011 Pb+Pb data at $\sqrt{s_{NN}} = 2.76$ TeV collected by the ATLAS detector [2].

The first evidence of the jet quenching at LHC has been observed in the measurement of the di-jet asymmetry [3]. In central heavy ion collisions an excess of events with large di-jet asymmetry has been observed when compared to p+p or Pb+Pb Monte Carlo (MC) reference. This asymmetry has been accompanied by a balance in azimuth, that is jets in the di-jet system remain “back-to-back” despite to a sizable modification of their energy. This measurement is an observation measurement and by itself it is insufficient to provide detailed information about the parton energy loss. To gain more information we need to ask more detailed questions: We need to know how does the modification of the inclusive jet spectra depend on the jet p_T , jet size, or direction of the jet with respect to the reaction plane. We also need to know whether the suppression depends on the flavor of the initial parton. Last but not least we should learn how is the internal structure of jets modified. These questions will be addressed in the sections 4-7. Section 2 summarizes the event selection and centrality definition, section 3 discusses the jet reconstruction performance.

¹A list of members of the ATLAS Collaboration and acknowledgements can be found at the end of this issue.

2. Event selection and centrality definition

Analyses presented in this summary use 2010 or 2011 LHC heavy ion runs, colliding nuclei at $\sqrt{s_{NN}} = 2.76$ TeV. The 2010 run collected approximately $7 \mu\text{b}^{-1}$ whereas 2011 run collected 0.14 nb^{-1} . Minimum bias Pb+Pb collisions were identified using measurements from the zero-degree calorimeters (ZDCs) and the minimum-bias trigger scintillator (MBTS) counters². In the offline analysis, events were required to have a primary vertex reconstructed from charged particle tracks with $p_T > 500$ MeV. The 2010 data-taking used only the minimum bias trigger whereas the in the 2011 run, events were selected for recording using a combination of the minimum bias trigger and high-level trigger (HLT). The HLT triggered on jets, high- p_T photons, electrons, and muons.

The centrality of each heavy ion collision is determined using the sum of the transverse energy in all cells in the forward calorimeter ($3.1 < |\eta| < 4.9$), at the electromagnetic scale. The average number of nucleon-nucleon collisions, N_{coll} , and the average number of participating nucleons, N_{part} , were calculated using the standard MC Glauber model [4].

3. Jet reconstruction performance

Jets discussed in this summary has been reconstructed at the calorimeter level using the anti- k_T algorithm [5]. The elliptic flow modulated underlying event contribution to the reconstructed jets has been subtracted on the event-by-event basis. All the discussed measurements have been corrected to the particle level by unfolding procedures such that they can be directly compared to theoretical models.

To evaluate the combined performance of the ATLAS detector and the jet reconstruction procedures the MC PYTHIA [7] di-jet events were embedded into HIJING [8] minimum bias events. The reference PYTHIA “truth” jets were reconstructed using the PYTHIA final-state particles by the anti- k_T algorithm with different radius parameters of $R = 0.2, 0.3, 0.4$, and 0.5 . Separately, the presence and approximate kinematics of HIJING-generated jets were obtained by running $R = 0.4$ anti- k_T reconstruction on final-state HIJING particles having $p_T > 4$ GeV. To prevent the overlap of PYTHIA and HIJING jets from distorting the jet performance evaluated relative to PYTHIA truth jets, all PYTHIA truth jets within $\Delta R = \sqrt{\Delta\eta^2 + \Delta\phi^2} = 0.8$ of a $p_T > 10$ GeV HIJING jet were excluded from the analysis. To eliminate jets originating from the underlying event fluctuations (“UE-jets”) the calorimeter jets were required to match a jet reconstructed from inner detector tracks or an electromagnetic cluster³.

PYTHIA truth jets passing the HIJING-jet exclusion were matched to the closest reconstructed jet of the same R value within $\Delta R = 0.2$. The resulting matched jets were used to evaluate the jet energy resolution (JER) and the jet energy scale (JES). The jet reconstruction efficiency is defined as the fraction of truth jets for which a matching reconstructed jet is found. The efficiency was evaluated both prior to (ϵ) and following (ϵ') UE-jet rejection described above. Figure 1 shows a summary of the jet reconstruction performance for anti- k_T $R = 0.2$ and $R = 0.4$ jets.

²The ZDCs are located symmetrically at $z = \pm 140$ m from the interaction point and cover $|\eta| > 8.3$. In Pb+Pb collisions the ZDCs primarily measure “spectator” neutrons, that is neutrons from the incident nuclei that do not interact hadronically. The MBTS measures charged particles over $2.1 < |\eta| < 3.9$.

³ Inner detector track jets were reconstructed by the anti- k_T $R = 0.4$ algorithm from tracks with $p_T > 4$ GeV and were required to have $p_T > 7$ GeV. Electromagnetic clusters were reconstructed from cells in the electromagnetic calorimeter and were required to have $p_T > 7$ GeV.

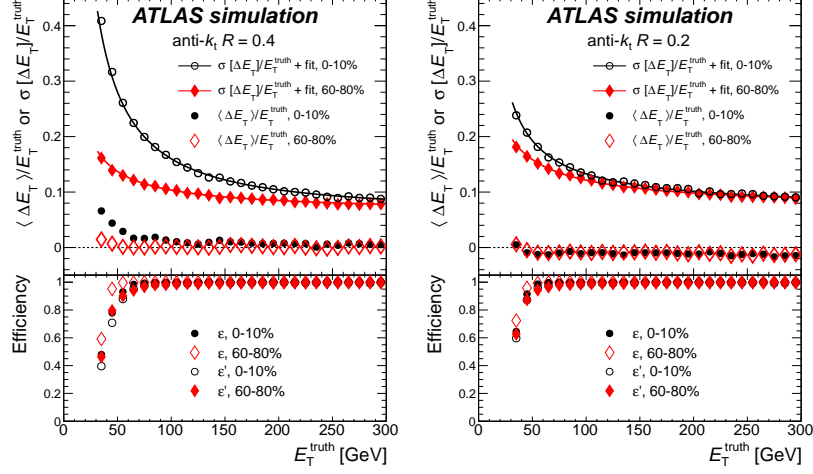


Figure 1: Results of MC evaluation of jet reconstruction performance in 0-10% and 60-80% collisions as a function of truth jet E_T for $R = 0.2$ (left) and $R = 0.4$ (right) jets [6]. *Top*: jet energy resolution $\sigma[\Delta(E_T)]/E_T^{\text{truth}}$ and jet energy scale closure $\langle\Delta E_T/E_T^{\text{truth}}\rangle$. Solid curve show the parametrization of the JER as described in the text. *Bottom*: Efficiencies, ϵ and ϵ' , for reconstructing jets before and after application of UE-jet removal, respectively.

The JER was characterized by $\sigma[\Delta(E_T)]/E_T^{\text{truth}}$, where $\sigma[\Delta(E_T)]$ is the standard deviation of the $\Delta E_T = E_T^{\text{reco}} - E_T^{\text{truth}}$ distribution. The JES closure was evaluated from the mean fractional energy shift, $\langle\Delta E_T/E_T^{\text{truth}}\rangle$. The JER was found to be well described by a quadrature sum of three terms,

$$\sigma[\Delta(E_T)]/E_T^{\text{truth}} = a/\sqrt{E_T^{\text{truth}}} \oplus b/E_T^{\text{truth}} \oplus c, \quad (1)$$

where a and c represent the usual sampling and constant contributions to calorimeter resolution. The term containing b describes the contribution of the underlying event fluctuations to the JER. This contribution can be independently evaluated by measuring the transverse energy fluctuations in the minimum bias events. This has been done in the fluctuation analysis reported in Ref. [9]. A good consistency between the results of the fluctuation analysis and the parametrization of the JER has been achieved. Simultaneously, a good agreement between the fluctuations in the data and HIJING has been observed.

The jet reconstruction efficiency decreases with decreasing jet E_T for $E_T \lesssim 50$ GeV. The decrease starts at larger E_T and decreases more rapidly for larger jet radii and in more central collisions. An independent check of the basic performance has been done by using PYTHIA jets embedded directly to the minimum bias data. The reconstruction efficiency was found to differ between central and peripheral collisions by less than 5% on the rise of the efficiency curve for $R = 0.4$ jets and the agreement in the JES was found to be better than a 1% between central and peripheral collisions. More details about the jet reconstruction procedures as well as the jet performance can be found in Ref. [6].

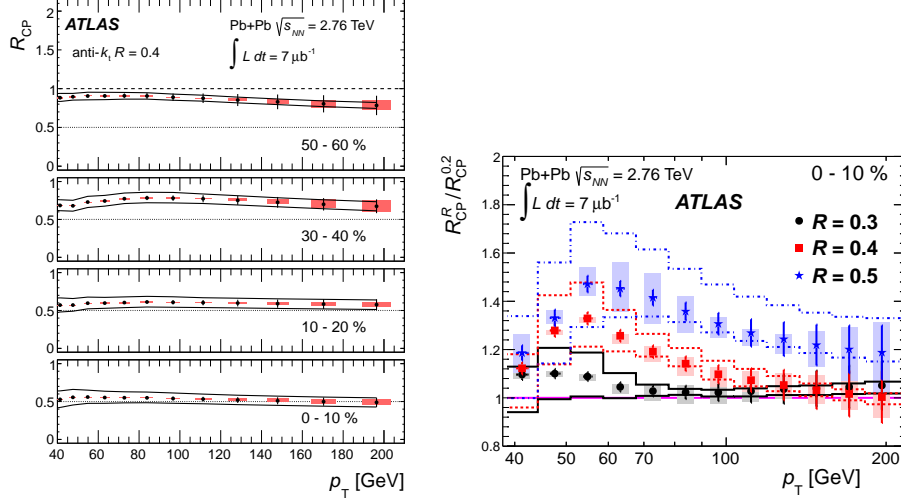


Figure 2: *Left:* Jet R_{CP} values as a function of jet p_T for $R = 0.4$ anti- k_T jets in two bins of collisions centrality. *Right:* Ratios of jet R_{CP} values between $R = 0.3, 0.4$, and 0.5 jets and $R = 0.2$ jets as a function of p_T in the 0-10% centrality bin. In both panels, the error bars show statistical uncertainties, shaded boxes indicate partially correlated systematic errors. The lines indicate systematic errors that are fully correlated between different p_T bins [6].

4. Inclusive jet suppression

The first step beyond the original asymmetry measurement is to measure the suppression in the inclusive jet yields. To quantify the suppression we introduce the jet R_{CP} , defined as a fraction of per-event normalized jet yield, \hat{N} , measured in a given centrality bin to the per-event normalized jet yield measured in the 60-80% most peripheral collisions, that is

$$R_{CP}^{\text{cent}} = (1/R_{\text{coll}}^{\text{cent}})(\hat{N}^{\text{cent}}/\hat{N}^{60-80}), \quad (2)$$

where $R_{\text{coll}}^{\text{cent}}$ is the central-to-peripheral ratio of number of binary collisions. The jet R_{CP} has been measured for six centrality bins, $\text{cent} \in \{0-10\%, 10-20\%, 20-30\%, 30-40\%, 40-50\%, 50-60\%\}$. The resulting jet R_{CP} evaluated as a function of jet p_T for 0-10% central and 50-60% peripheral collisions is presented in the left panel of Figure 2. One can see that the jet R_{CP} in the most central collision does not exhibit any strong dependence on the jet p_T . A suppression by a factor of two of inclusive jet yields in 0-10% central with respect to 60-80% peripheral collisions can be observed.

The dependence of the jet suppression on the jet size is summarized in the right panel of Figure 2 in terms of the ratio of R_{CP} values between $R = 0.3, 0.4$, and 0.5 jets and $R = 0.2$ jets, $R_{CP}^R / R_{CP}^{0.2}$, as a function of p_T for the 0-10% centrality bin. This result indicates a significant dependence of R_{CP} on the jet radius. For $p_T < 100$ GeV the $R_{CP}^R / R_{CP}^{0.2}$ values for both $R = 0.4$ and $R = 0.5$ differ from one beyond the statistical and systematic uncertainties. This deviation persists well beyond 100 GeV and is also present in 10-20% centrality bin. However, the direct comparisons of R_{CP} between different jet radii at low p_T should be treated with care as the same jets measured using smaller radii will tend to appear in lower p_T bins than when measured with a larger radius. Further details on the inclusive jet suppression can be found in Ref. [6].

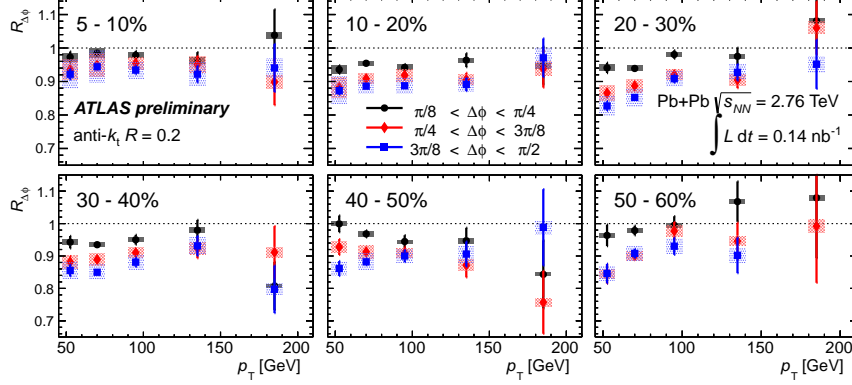


Figure 3: Azimuthal dependence of the jet suppression measured in terms of $R_{\Delta\phi}$ as a function of jet p_T for three bins of the angle to the elliptic flow event plan, $\Delta\phi$, evaluated relative to the $0 < \Delta\phi < \pi/8$. Error bars show statistical uncertainties, shaded boxes indicate systematic uncertainties [11].

To get more insight into the dependence of the jet suppression on the path length the original parton would have traversed through the medium the variation of inclusive jet yields as a function of azimuthal angle, $\Delta\phi$, with respect to the elliptic flow event plane was measured. This variation can be quantified using the ratio of jet yield in one $\Delta\phi$ bin i to another j , $R_{\Delta\phi}$, defined by

$$R_{\Delta\phi} = \frac{Y(p_T, \phi)|_{\Delta\phi=\Delta\phi_i}}{Y(p_T, \phi)|_{\Delta\phi=\Delta\phi_j}} = \frac{\frac{d^2 N(p_T, \phi)}{dp_T d\phi}|_{\Delta\phi=\Delta\phi_i}}{\frac{d^2 N(p_T, \phi)}{dp_T d\phi}|_{\Delta\phi=\Delta\phi_j}} \quad (3)$$

where the jet yield $Y(p_T, \phi)$ is measured in four $\Delta\phi$ bins spanning equidistantly the range $0 < \Delta\phi < \pi/2$. The resulting $R_{\Delta\phi}$ distributions plotted as a function of jet p_T are shown in Figure 3. A clear reduction of the jet yield with increasing $\Delta\phi$ is observed. For example, in the 20-30% centrality bin, jets produced in the direction perpendicular to the elliptic flow event plane ($3\pi/8 < \Delta\phi < \pi/2$) are suppressed by $\approx 15\%$ with respect to jets produced in the direction of the elliptic flow plane ($0 < \Delta\phi < \pi/8$). Another way to quantify the azimuthal dependence of the jet suppression is to measure the elliptic flow parameter of jets, v_2^{jet} . The v_2^{jet} was found to decrease with increasing centrality and to have a characteristic centrality dependence known from elliptic flow measurements of single particles [10]. The v_2^{jet} reaches its maximum of $\approx 0.04 - 0.05$ in mid-central collisions ($N_{part} = 100 - 200$) for jets with $p_T = 45 - 60$ GeV. More details on the azimuthal dependence of inclusive jet suppression can be found in Ref. [11].

5. Photon-jet and Z^0 -jet correlations

The fact that the measured jet suppression at LHC is not an effect of initial state modifications was proven by the measurement of inclusive yields of prompt photons [12] and inclusive yields of W^\pm, Z^0 vector bosons [13, 14] which do not exhibit any suppression in central heavy ion collisions. Since photons and vector bosons are insensitive to the colored medium they can provide means to calibrate the expected energy of quenched jet in a photon-jet system or in a Z^0 -jet system. The quenching of the jet in the photon-jet sample can be quantified by measuring

the jet to photon energy ratio, $x_{J\gamma} = p_T^{jet}/p_T^\gamma$. The left panel of Figure 4 shows the integrated per-photon jet yield, $R_{J\gamma}$, evaluated as a function of the number of participants for data and MC. A clear suppression of the jet yield is seen in central compared to peripheral collisions. The measurement is performed for two different jet sizes, $R = 0.2$ and $R = 0.3$ providing the same result within the systematic uncertainties. Qualitatively the same result has been obtained also from the Z^0 -jet correlation measurements in which the Z^0 have been identified from the e^+e^- and $\mu^+\mu^-$ decays. The same trend in the evolution of the jet suppression as a function of centrality has been observed despite to the limited statistics of less than forty Z^0 -jet events. These results provide a starting point for precision measurements of the jet quenching which will be allowed by future high luminosity heavy ion runs at LHC. More details on γ -jet correlations are provided in Ref. [15], details on Z^0 -jet correlations are provided in Ref. [16].

6. Heavy flavor suppression

To access the difference between the jet suppression of heavy quarks and light quarks the semi-leptonic decays of open heavy flavor hadrons into muons has been measured. The measurement was performed over the muon transverse momentum range $4 < p_T < 14$ GeV. Over this p_T range, muon production results predominantly from a combination of charm and bottom quark semi-leptonic decays. The differential yield of muons in a given centrality and p_T bin was compared to that in a peripheral bin through the central-to-peripheral ratio, R_{CP} . The right panel of Figure 4 shows a comparison of the muon R_{CP} as a function of centrality for four different p_T intervals. One can see a smooth decrease in the R_{CP} with increasing centrality. The suppression does not change with the muon p_T while the size of the suppression changes by nearly a factor of two between the most central and the most peripheral bins. A similar size of suppression between the yields of muons from semi-leptonic heavy quark decays and inclusive jet yields together with the R_{CP} of muons being rather flat as a function of p_T suggests no dramatic difference between the light and heavy quark response to the medium. More details on the heavy flavor suppression are provided in Ref. [17].

7. Jet fragmentation

One of the tools that allow precise comparison between the data and theoretical models of jet quenching is the measurement of jet fragmentation.

The key question to address is how are the parton showers modified by the medium. To provide an experimental answer to this question we measure the p_T spectra of charged particles inside jets, $D(p_T)$, and the jet fragmentation function, $D(z)$, defined as

$$D(p_T) \equiv \frac{1}{N_{jet}} \frac{1}{\varepsilon} \frac{\Delta N_{ch}(p_T)}{\Delta p_T} \quad (4)$$

$$D(z) \equiv \frac{1}{N_{jet}} \frac{1}{\varepsilon} \frac{\Delta N_{ch}(z)}{\Delta z} \quad (5)$$

where N_{jet} represents the total number of measured jets in the given centrality bin, $\Delta N_{ch}(p_T)$ and $\Delta N_{ch}(z)$ represent the number of measured charged particles within $\Delta R = 0.4$ of the jets in given bins of p_T and z , respectively, and ε represents the MC-evaluated p_T and pseudorapidity dependent reconstruction efficiency. The fragmentation variable, z , is defined as a ratio of charged

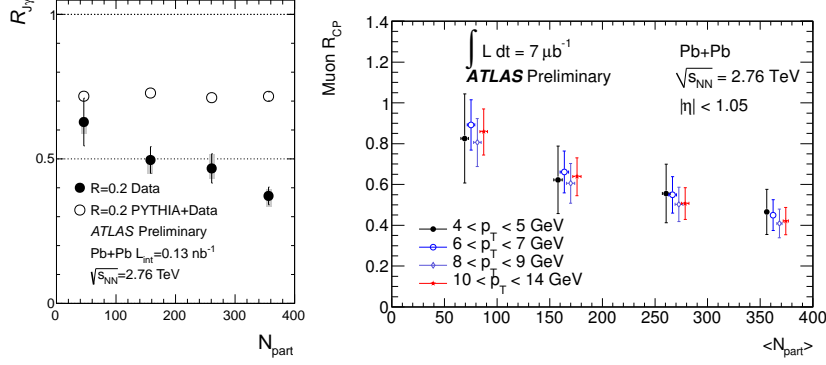


Figure 4: *Left*: The integrated yield of jets per photon, $R_{J\gamma}$, calculated as a function of number of participating nucleons, N_{part} . The kinematic cuts are: photon $60 < p_T^\gamma < 90$ GeV, $|\eta^\gamma| < 1.3$, $p_T^{\text{jet}} > 25$ GeV, $|\eta^{\text{jet}}| < 2.1$. The azimuthal distance between jet and photon is required to be $|\Delta\phi_{J\gamma}| > 7\pi/8$. The error bars represent statistical errors, while the gray bands indicate the systematic uncertainties [15], [16]. *Right*: Muon R_{CP} as a function of N_{part} calculated for different bins in muon p_T . The sets of points for the different p_T bins are successively displaced by $\Delta N_{\text{part}} = 6$ for clarity of presentation. The error bars represent combined statistical and systematic uncertainties [17].

particle momentum to the momentum of associated jet, $z = p_T^{\text{trk}}/p_T^{\text{jet}} \cos \Delta R$, where ΔR is the distance between the jet axis and a charged particle. The underlying event contribution to the $D(z)$ and $D(p_T)$ distributions is determined on the jet-by-jet basis and subtracted from the measured distributions. Jet fragmentation has been measured for three different jet radius parameters, $R = 0.4, 0.3$, and 0.2 providing quantitatively the same result. The ratio of central to 60-80% peripheral collisions of $D(p_T)$ distributions, $R_{D(p_T)}$, and $D(z)$ distributions, $R_{D(z)}$, is calculated. The $R_{D(p_T)}$ and $R_{D(z)}$ has been measured for six centrality bins, 0-10%, 10-20%, 20-30%, 30-40%, 40-50%, and 50-60%. The resulting distributions for $R = 0.4$ jets and 0-10% centrality bin are plotted in Figure 5. The ratios show a reduction of fragment yield in all centrality bins relative to the 60-80% bin at intermediate z values, $0.05 \lesssim z \lesssim 0.2$ and an enhancement in fragment yield for $z \lesssim 0.05$. No significant modification is seen in $D(z)$ or $D(p_T)$ distributions at high p_T or z . The reduction in the yield at intermediate z decreases gradually from central to peripheral collisions. More details on the jet fragmentation measurement is provided in Ref. [18].

The picture of the jet fragmentation at high- p_T is consistent with both the inclusive jet suppression and suppression of single charged particles reported in Ref. [19]. The charged particle R_{CP} achieves a value of ≈ 0.6 , that is a similar value as the R_{CP} of inclusive jets. Since the R_{CP} of inclusive jets is rather flat as a function jet p_T and since all the measured charged particles at high- p_T should be also measured in jets we can expect no significant modification of yields of high- p_T fragments between central and peripheral collisions. This is indeed seen in the measurement of the jet fragmentation.

8. Summary

We have presented results of the measurement of inclusive jet suppression, azimuthal dependence of jet suppression, jet suppression in γ -jet and Z^0 -jet system, suppression of heavy flavor, and jet fragmentation. We find that the inclusive jet yields are suppressed by approximately a factor of two in central compared to peripheral collisions. This suppression has only a weak

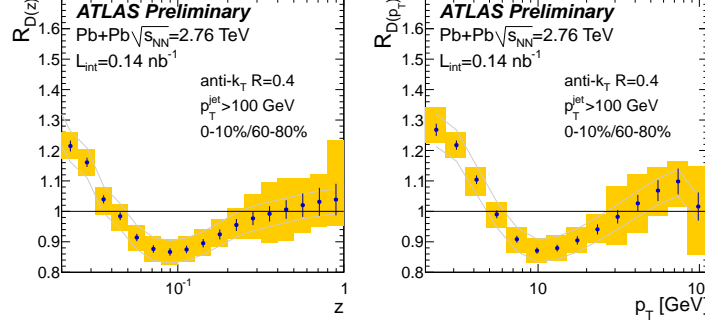


Figure 5: *Left:* Ratio of fragmentation functions, $R_{D(z)}$. *Right:* Ratio of p_T spectra of charged particles inside jets, $R_{D(p_T)}$. Both $R_{D(z)}$ and $R_{D(p_T)}$ are ratios of 0-10% central to 60-80% peripheral events evaluated for $R = 0.4$ anti- k_T jets. The error bars on the data points show statistical uncertainties, the shaded bands indicate systematic uncertainties that are uncorrelated or partially correlated between points. The solid lines indicate systematic uncertainties that are 100% correlated between points [18].

dependence on the jet p_T . A significant dependence of the jet suppression on the jet size is seen – with increasing jet radius the suppression is weaker. The jet suppression depends on the direction of the jet with respect to elliptic flow event plane. A maximal difference of $\approx 15\%$ in the jet yields for jets produced in plane compared to jets produced perpendicular to the elliptic flow plane is observed. The jet suppression is also observed in γ -jet and Z^0 -jet systems. The measurement of semi-leptonic decays of open heavy flavor hadrons to muons suggests a similar suppression of heavy quark jets and light quark jets. The jet fragmentation function and momentum spectra of charged particles produced inside jets are modified in central compared to peripheral collisions. The yield of low- z fragments is enhanced whereas the yield of intermediate z fragments is suppressed. No sizable difference of high- z fragments is seen.

References

- [1] A. Majumder, M. Van Leeuwen, Prog. Part. Nucl. Phys. A66 (2011) 41–92.
- [2] ATLAS Collaboration, JINST 3 (2008) S08003.
- [3] ATLAS Collaboration, Phys. Rev. Lett. 105 (2010) 252303.
- [4] B. Alver, M. Baker, C. Loizides, P. Steinberg, arXiv:0805.4411.
- [5] M. Cacciari, G. P. Salam, G. Soyez, JHEP 04 (2008) 063.
- [6] ATLAS Collaboration, arXiv:1208.1967.
- [7] T. Sjostrand, S. Mrenna, P. Z. Skands, JHEP 05 (2006) 026.
- [8] X.-N. Wang, M. Gyulassy, Phys. Rev. D44 (1991) 3501–3516.
- [9] ATLAS Collaboration, ATLAS-CONF-2012-045.
- [10] ATLAS Collaboration, Phys. Lett. B707 (2012) 330–348.
- [11] ATLAS Collaboration, ATLAS-CONF-2012-116.
- [12] ATLAS Collaboration, ATLAS-CONF-2012-051.
- [13] ATLAS Collaboration, ATLAS-CONF-2011-078.
- [14] ATLAS Collaboration, ATLAS-CONF-2012-052.
- [15] ATLAS Collaboration, ATLAS-CONF-2012-121.
- [16] ATLAS Collaboration, ATLAS-CONF-2012-119.
- [17] ATLAS Collaboration, ATLAS-CONF-2012-050.
- [18] ATLAS Collaboration, ATLAS-CONF-2012-115.
- [19] ATLAS Collaboration, ATLAS-CONF-2012-120.